ENZYMOLOGY

Capture of a third Mg^{2+} is essential for catalyzing DNA synthesis

Yang Gao and Wei Yang*

It is generally assumed that an enzyme-substrate (ES) complex contains all components necessary for catalysis and that conversion to products occurs by rearrangement of atoms, protons, and electrons. However, we find that DNA synthesis does not occur in a fully assembled DNA polymerase–DNA–deoxynucleoside triphosphate complex with two canonical metal ions bound. Using time-resolved x-ray crystallography, we show that the phosphoryltransfer reaction takes place only after the ES complex captures a third divalent cation that is not coordinated by the enzyme. Binding of the third cation is incompatible with the basal ES complex and requires thermal activation of the ES for entry. It is likely that the third cation provides the ultimate boost over the energy barrier to catalysis of DNA synthesis.

Enzymes increase the rate of chemical reactions, which is thought to occur by a reduction in the activation energy required to reach the transition state (Fig. 1A) (*1*–*3*). Because of their transient and unstable nature, authentic transition states have not been visualized but are assumed to have the same chemical components as the substrate state. DNA polymerases, which catalyze a phosphoryltransfer reaction that incorporates deoxynucleoside triphosphates (dNTPs) into DNA, are known to require two Mg^{2+} ions (Fig. 1B) (*4*–*8*). Despite extensive kinetic studies using the stopped-flow technique and the dNTP analog dNTPαS, it remains controversial whether a conformational transition before catalysis (*9*–*14*) or the chemistry itself (*15*, *16*) is the rate-limiting step in DNA synthesis.

Do not quite understand this.

Laboratory of Molecular Biology, National Institute of Diabetes and Digestive and Kidney Diseases, National Institutes of Health, Bethesda, MD 20892, USA.
*Corresponding author. Email: wei.yang@nih.gov

We have recently visualized phosphodiester bond formation catalyzed by human DNA polymerase (Pol) η in crystallo (*17*). Consistent with the two–metal ion mechanism (*6*–*8*), binding of Mg^{2+} ions in the A and B sites occurs within 40 s and leads to alignment of the 3′-OH of the primer end with the α-phosphate of dNTP (Fig. 1C) (*17*). After another 40 s, product starts to appear without discernible conformational change of the enzyme or substrates. However, we observed a third Mg^{2+} ion appearing in a third "C" site after product formation (Fig. 1C) (*17*). An equivalent third metal ion, coordinated by the reaction products and four water molecules, has also been observed in the in-crystallo catalysis by DNA Pol β (*18*–*20*). Because of steric clashes with dNTP (Fig. 1C), the third metal ion cannot bind in Pol η enzyme-substrate (ES) complexes. Because of low occupancy in the C site and weak diffraction of Mg^{2+} ions, it has been unclear when the third Mg^{2+} appears and whether it is involved in the phosphoryltransfer reaction.

To determine the reaction coordinates of Pol η and the role of the third metal ion, we replaced Mg^{2+} with Mn^{2+}, which supports DNA synthesis (*21*) and is readily detected by x-ray diffraction even at low occupancy. Crystals of native Pol η (1 to 432 amino acids) in complex with DNA, deoxyadenosine triphosphate (dATP), and Ca^{2+} were grown at pH 6.0 in a nonreactive ground state (*17*). After exposure to a pH 7.0 reaction buffer containing 1 mM Mn^{2+} for 90 to 1800 s, crystals were flash frozen in liquid N_2 to stop the reaction, and 1.5 to 1.7 Å x-ray structures were determined at five reaction time points (table S1 and Materials and Methods). All five structures were practically identical, except for the gradual replacement of Ca^{2+} by Mn^{2+} in the B site (fig. S1). By 600 s, when ~90% of the A and B sites were occupied by Mn^{2+}, the 3′-OH of the DNA primer was aligned with the α-phosphorus of the dATP, and the structure was identical to that of crystals soaked in 1 mM Mg^{2+} for 40 s (fig. S2, A and B). Similar to the reaction in Mg^{2+} (*17*), a water molecule (WatN) hydrogen bonded to the nucleophilic 3′-OH appeared at 90 s, and its occupancy increased with time in correlation with binding of the A-site Mn^{2+} (fig. S2, C and D). However, in 1 mM Mn^{2+}, the Pol η–DNA complex remained in the substrate state with no product and no C-site Mn^{2+} ion for up to 1800 s (Fig. 1D).

We assayed the metal ion (Me^{2+}) requirements for Pol η catalysis in solution and found that 0.6 mM Mg^{2+} or 2.7 mM Mn^{2+} is needed to attain the half-maximal reaction rate (Fig. 2A and table S2). We then examined the Mn^{2+} affinity of each binding site in crystallo. Although increasing the Mn^{2+} concentration (0.5 to 15 mM) accelerated the rate of metal-ion binding in all three sites (Fig. 2B and table S3), the apparent dissociation constant (K_d) values of the A and

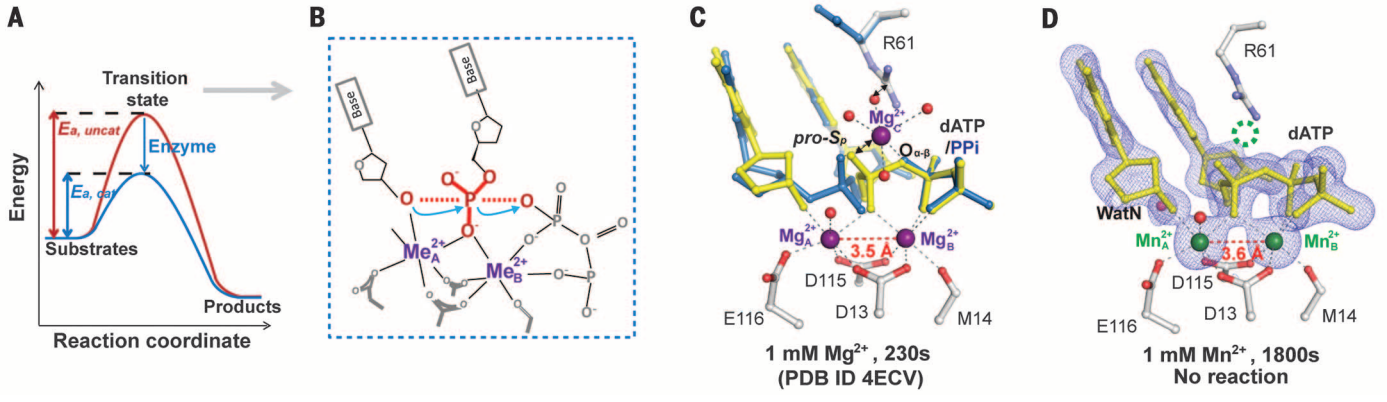

Fig. 1. No DNA synthesis without the third metal ion. (**A**) Reaction coordinate of enzyme catalysis. (**B**) The assumed transition state of the two–metal ion catalysis. (**C**) The structure of Pol η catalyzing DNA synthesis in crystallo (PDB: 4ECV) (*17*). The C-site Mg^{2+} is coordinated by the products (60%, blue) but clashes with the substrate dATP and R61 side chain (40%, yellow). (**D**) The structure of Pol η incubated with substrates and 1 mM Mn^{2+} for 1800 s. No C-site metal ion or reaction products were detected. The corresponding $F_{obs} - F_{calc}$ (F_o-F_c) omit map contoured at 3.5 σ (blue mesh) is superimposed.

B sites were below 0.5 mM. The K_d for the C site, however, was 3.2 mM, close to the 2.7 mM measured in solution (Fig. 2A).

When in-crystallo reactions occurred in 10 mM Mn^{2+}, catalysis proceeded as in 1 mM Mg^{2+} (*17*), except that the A-site Mn^{2+} did not dissociate upon product formation as does Mg^{2+} (fig. S3, A and B) and slightly less product accumulated with Mn^{2+} than with Mg^{2+}. However, unlike the reaction in Mg^{2+}, the C-site Mn^{2+} appeared simultaneously with the reaction product, 30 s after binding of the two canonical metal ions (Fig. 2C). Electron density for the new phosphodiester bond and the C-site Mn^{2+}, whose chemical nature was confirmed by its anomalous diffraction and characteristic octahedral coordination geometry (fig. S3C), had one-to-one correlation at every time point and Mn^{2+} concentration (Fig. 2D). In Mg^{2+} by contrast, with 15% product formed at 80 s, the C-site Mg^{2+} was at too low occupancy to be observed and was not detected until 140 s when product had accumulated to 40% (fig. S3A) (*17*). Previous stopped-flow studies indicate that one of the metal ion–binding sites has much lower affinity for Mg^{2+} and, thus, limits DNA synthesis (*16*). Our in-crystallo titrations unequivocally show that the low-affinity binding site is neither A nor B but the C site, which determines the concentration of Mg^{2+} or Mn^{2+} necessary for the DNA synthesis reaction.

The C-site Me^{2+} is coordinated by four water molecules and two oxygen atoms, one each from the product DNA and pyrophosphate, which correspond to the α pro-S_p oxygen and the α,β bridging oxygen of dNTP (Fig. 1C). Sulfur substitution of the pro-S_p oxygen (S_p-dNTPαS) has been widely used to dissect the reaction kinetics of DNA synthesis (*11–14*, *22*), because the pro-S_p atom is not directly involved in A- or B-site Me^{2+} coordination. The reduction of the reaction rate by S_p-dNTPαS has been interpreted to be "conformational" (for reduction of less than three-quarters) or to affect the chemistry itself (for a reduction of more than three quarters) (*11–14*, *23*).

As a ligand of the third Me^{2+}, the sulfur in S_p-dATPαS was tolerated by Pol η (table S2) but required much higher [Mg^{2+}] (15 mM) and [Mn^{2+}] (9 mM) than dATP for catalysis to occur (Figs. 2A and 3A). Unexpectedly, in-crystallo S_p-dATPαS slowed Mg^{2+} and Mn^{2+} binding at the A site. After a lengthened delay, product started to form, but the C site remained empty (Fig. 3B and fig. S4, A to C). We suspect that the third Mn^{2+} still assisted product formation, but the association was too transient to be observed. In addition, although A-site Mg^{2+} occupancy was reduced in the presence of dATPαS, an alternative A′ site appeared 2.6 Å away (fig. S4, D and E). These data suggest that the reduced reaction rate with S_p-dATPαS cannot be attributed to conformational effects (*11–14*) but involves impaired A- and C-site Mg^{2+} binding and altered reaction chemistry.

To bind the third Me^{2+}, the arginine 61 (R61) side chain, which forms salt bridges with the dNTP (*17*), moves to vacate the C site (Figs. 1C and 3B). When alanine replaces arginine at position 61 (R61A), the enzymatic rate (k_{cat}) is reduced by two-thirds (table S2) (*24*, *25*), but the metal-ion requirement and the general reaction process in crystallo were indistinguishable from wild-type (WT) Pol η (fig. S5, E and F). However, the delay between binding of two Mg^{2+} ions and product formation was lengthened from WT's 40 s to R61A's 160 s (Fig. 3C). This delay likely stems from a slight shift of dATP away from the active site and a 0.3 Å increase in separation between the 3′-OH and α-phosphate (Fig. 3D). The void left by the R61A mutation was occupied by water molecules (*25*) and not by the abundant K^+ or Rb^+ (identifiable by anomalous diffraction) in the reaction buffer (fig. S5). The subtle misalignment of the substrate, which was repeatedly observed with R61A and R61M (in which methionine replaces Arg^{61}) mutant Pol η (*25*) and with dATPαS, led to a prolonged delay before C-site Me^{2+} binding and product formation (fig. S4, B and C).

Notably, a +1 charged side chain at the position equivalent to R61 is found in all A-, B-, and Y-family DNA polymerases and reverse transcriptases, despite diverse structures of finger domains surrounding the C site (fig. S6). Among C- and X-family DNA polymerases, there is no R61 equivalent, but the third metal ion has been observed for the X-family Pol β (*18–20*). The finger domains, which carry the +1 charged residue, distinguish correct from incorrect incoming nucleotides by enclosing only a correct dNTP (*26*). A closed finger appears to be a prerequisite for C-site metal-ion binding and catalysis. The varied environment surrounding the C site may thus be exploited for drug design to increase specificity and to reduce toxicity of broadly used nucleoside and nucleotide analogs targeting DNA polymerases in antiviral and anticancer therapeutics (*27*, *28*).

Because the C site does not exist in the Pol η–substrate complex but is required for product formation, we hypothesized that thermal motion of the well-aligned reactants in the ES complex may create an opening for the third metal ion. If so, elevated temperature would promote C-site metal-ion binding and thus catalysis. To test this hypothesis, we designed a two-step in-crystallo reaction. The Pol η crystals were first soaked in 1 mM Mn^{2+} to saturate the A and B sites and then exposed to 5 mM Mn^{2+} at 4°C to 37°C for 60 s for catalysis to occur (Fig. 4A). The diffusion rate of Mn^{2+} in crystallo was unaffected by temperature, as demonstrated by Mn^{2+} binding at the A site (Fig. 4B). But in the two-step reaction, no C-site Mn^{2+} or product was detected at 4°C (Fig. 4C). At 14°C, low levels of the third Mn^{2+} ion and products were observed, and their

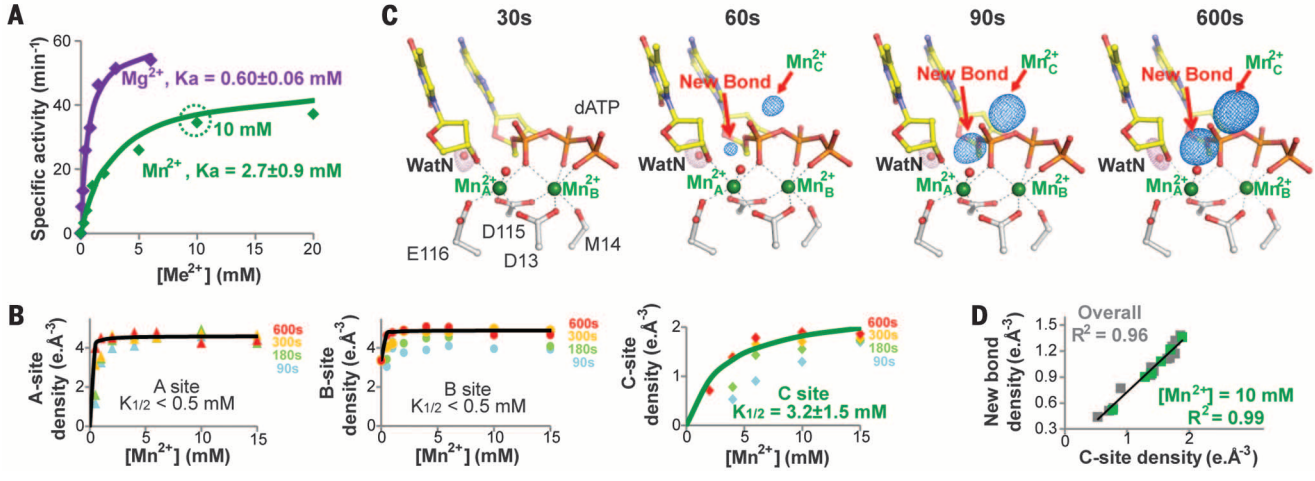

Fig. 2. Coupled appearance of the third Mn^{2+} and reaction products. (**A**) Mg^{2+} (purple) and Mn^{2+} (green) dependence of Pol η catalysis in solution. K_a, activation constant. (**B**) Titration of the A-, B-, and C-site Mn^{2+} binding in crystallo. The 600-s data were fitted to equilibrium binding modes to yield the K_d values. (**C**) Structures of Pol η in-crystallo catalysis with 10 mM Mn^{2+}. The F_o-F_c omit map for the new bond, the C-site Mn^{2+} (blue) and the WatN (pink) were contoured at 3σ and superimposed onto each structure. (**D**) Correlation (R^2) between the new bond formation and the C-site Mn^{2+} binding.

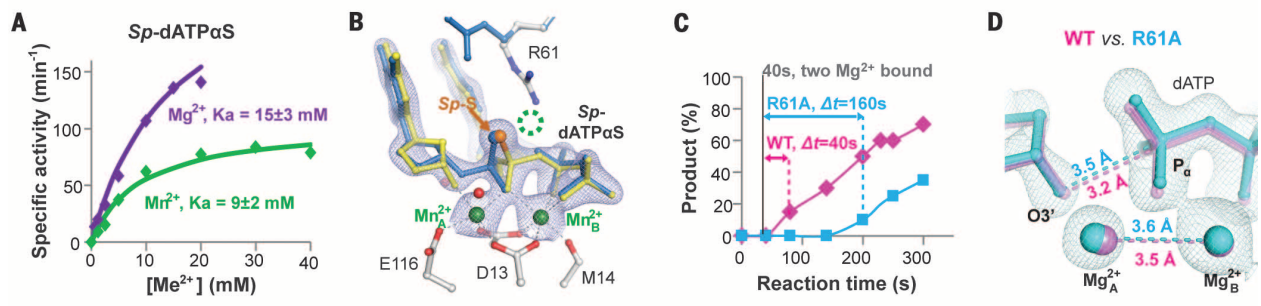

Fig. 3. Changing the C-site environment alters Pol η catalysis. (**A**) Mg^{2+} (purple) and Mn^{2+} (green) dependence of Pol η incorporating dATPαS in solution. (**B**) In crystallo incorporation of dATPαS by Pol η with 20 mM Mn^{2+} at 600 s showed product formation (50%) but no C-site Mn^{2+}. The $2F_o$-F_c map contoured at 2σ level (blue meshes) is superimposed. (**C**) Time delay in product formation by WT (magenta) and R61A (cyan) Pol η in crystallo. (**D**) Deviation of dATP in the ES of R61A Pol η [cyan with $2F_o$-F_c map contoured at 1.5σ] from WT Pol η (magenta).

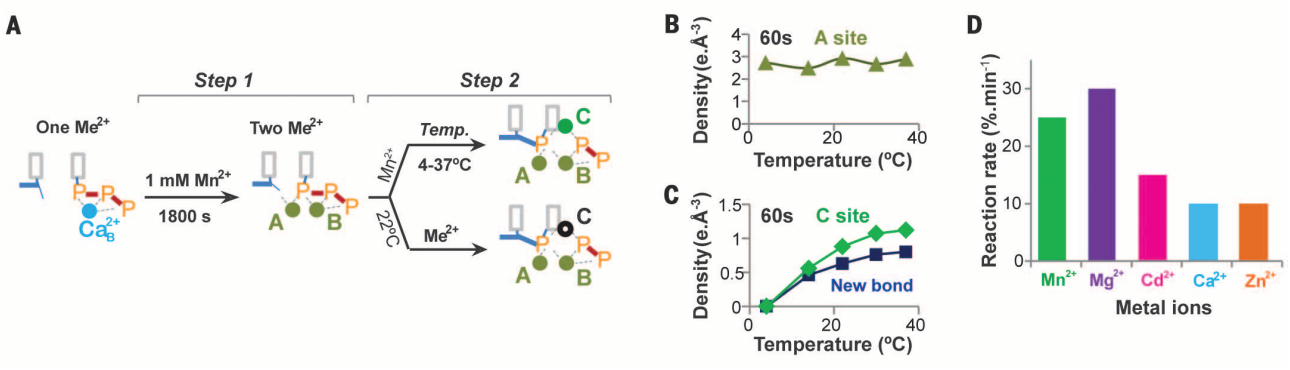

Fig. 4. Thermal energy-dependent C-site formation and its metal-ion selectivity. (**A**) Schematic diagram of the two-step in-crystallo reactions that probe the C-site formation and ion selectivity. (**B**) Binding of the A-site Mn^{2+} was unaffected by varying temperature from 4°C to 37°C. (**C**) Binding of the C-site Mn^{2+} and the product formation increased with the temperature from 4°C to 37°C. (**D**) Rates of product formation with five metal ions tested in the second step.

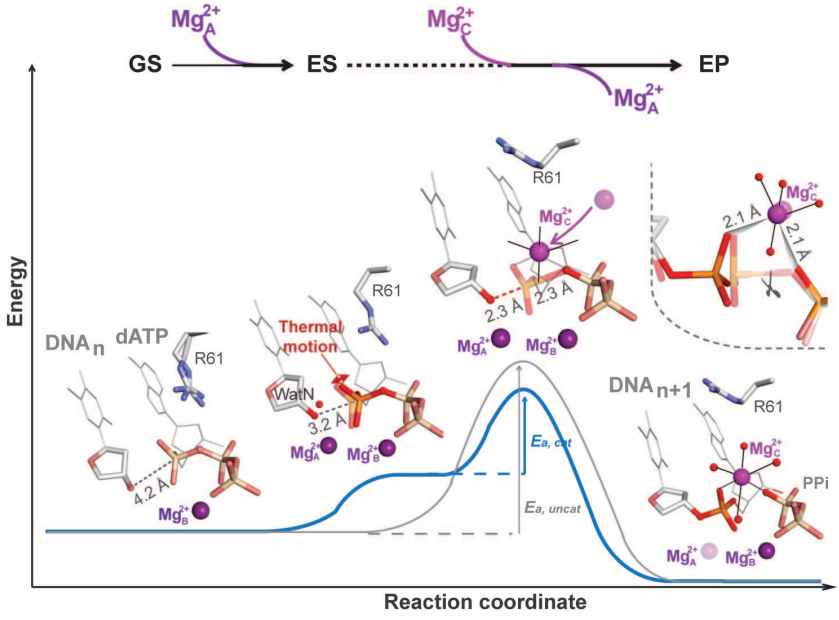

Fig. 5. Mechanism of Pol η catalysis. Pol η binds DNA and an incoming dNTP along with the B-site Mg^{2+} to form the ground state (GS). Binding of the A-site Mg^{2+} leads to the reaction-ready ES state, in which the 3′-OH is aligned with dNTP and WatN is recruited. Thermal motions of the reactants create the C site, which leads to the third metal-ion binding and the transition state (TS) formation. The C-site metal ion promotes the phosphoryltransfer from the leaving group to the nucleophilic 3′-OH by which it overcomes the energy barrier to the product state (PS). E_a, the activation energy of the reaction, catalyzed or uncatalyzed.

amounts doubled at 30°C. The temperature dependence of C-site and product formation corroborates that binding of the third metal ion is rate limiting in the DNA synthesis reaction.

To determine the metal-ion selectivity at the C site, we varied Me^{2+} in the second step of the two-step reaction (Fig. 4A). Catalysis occurred most efficiently with Mg^{2+}, followed by Mn^{2+} and Cd^{2+} (Fig. 4D and fig. S7). Ca^{2+} and Zn^{2+} seemingly also led to product formation at ~40% efficiency of Mg^{2+}. However, the C-site coordination geometry with all five Me^{2+} tested appeared identical to that of Mg^{2+} and Mn^{2+} (fig. S7), despite different coordination distances of Ca^{2+} (2.3 to 2.5 Å) and Mg^{2+} or Mn^{2+} (2.1 Å). It is thus likely that Ca^{2+} and Zn^{2+} replaced A- or B-site Mn^{2+} in some Pol η molecules and that the freed Mn^{2+} ions may occupy the C site in other Pol η molecules to support the catalysis. The low affinity and strong preference for Mg^{2+} at the C site, which cannot be explained by its coordination ligands, suggest a catalytic role for the third metal ion in DNA synthesis.

On the basis of the requirement for three metal ions in DNA synthesis, we suggest a revision of the catalytic mechanism (Fig. 5). DNA synthesis begins with binding of dNTP along with the B-site Mg^{2+} and formation of a ground-state Pol η–DNA-dNTP-Mg^{2+} complex (GS). Watson-Crick pairing between the template and dNTP

favors A-site Mg^{2+} binding. The two Mg^{2+} ions and the R61 side chain neutralize and align dNTP with DNA in the reaction-ready state (ES), where the juxtaposed and polarized substrates recruit WatN (fig. S2) (*17*). However, neither deprotonation nor chemistry takes place without the C-site Mg^{2+}. Thermal motion may transiently bring the perfectly aligned reactants closer to each other by fractions of an angstrom and may create an entry for the third Mg^{2+}. Close approach of the reactants may also increase negative charge around the α-phosphate and favor replacement of the +1 charged R61 by the C-site Mg^{2+}. We hypothesize that the energy barrier to the transition state is overcome by binding of the third Mg^{2+}. The stringent octahedral coordination geometry of Mg^{2+} implies that the C-site Mg^{2+} may help to break the α-β phosphodiester bond (Fig. 5) in addition to protonating the pyrophosphate leaving group (*17*). Product formation is coupled to disappearance of WatN (fig. S3D), which likely deprotonates the 3′-OH, and to release of the A-site Mg^{2+}, which prevents the reverse reaction (fig. S3, A and B).

It has long been assumed that enzymes stabilize transition states and reduce the energy barrier to product formation (Fig. 1A), but de novo design of enzymes based on this assumption has not been successful (*29*–*32*). Notwithstanding its crucial role in catalysis, the C-site metal ion of polymerases has evaded detection by biochemical and structural studies of DNA polymerases for decades. Identification of the essential third metal ion in the Pol η catalysis leads us to anticipate that acquisition of transient metal-ion cofactors in transition states may be a general feature that enables enzyme catalysis.

REFERENCES AND NOTES

1. M. Garcia-Viloca, J. Gao, M. Karplus, D. G. Truhlar, *Science* **303**, 186–195 (2004).
2. S. J. Benkovic, S. Hammes-Schiffer, *Science* **301**, 1196–1202 (2003).
3. A. Warshel *et al.*, *Chem. Rev.* **106**, 3210–3235 (2006).
4. P. J. Rothwell, G. Waksman, *Adv. Protein Chem.* **71**, 401–440 (2005).
5. M. D. Tsai, *Biochemistry* **53**, 2749–2751 (2014).
6. T. A. Steitz, J. A. Steitz, *Proc. Natl. Acad. Sci. U.S.A.* **90**, 6498–6502 (1993).
7. T. A. Steitz, *J. Biol. Chem.* **274**, 17395–17398 (1999).
8. W. Yang, J. Y. Lee, M. Nowotny, *Mol. Cell* **22**, 5–13 (2006).
9. C. M. Joyce, S. J. Benkovic, *Biochemistry* **43**, 14317–14324 (2004).
10. K. A. Johnson, *J. Biol. Chem.* **283**, 26297–26301 (2008).
11. S. S. Patel, I. Wong, K. A. Johnson, *Biochemistry* **30**, 511–525 (1991).
12. M. E. Dahlberg, S. J. Benkovic, *Biochemistry* **30**, 4835–4843 (1991).
13. M. T. Washington, L. Prakash, S. Prakash, *Cell* **107**, 917–927 (2001).
14. K. A. Fiala, Z. Suo, *Biochemistry* **43**, 2116–2125 (2004).
15. P. J. Rothwell, V. Mitaksov, G. Waksman, *Mol. Cell* **19**, 345–355 (2005).
16. M. Bakhtina *et al.*, *Biochemistry* **44**, 5177–5187 (2005).
17. T. Nakamura, Y. Zhao, Y. Yamagata, Y. J. Hua, W. Yang, *Nature* **487**, 196–201 (2012).
18. B. D. Freudenthal, W. A. Beard, D. D. Shock, S. H. Wilson, *Cell* **154**, 157–168 (2013).
19. B. D. Freudenthal *et al.*, *Nature* **517**, 635–639 (2015).
20. R. Vyas, A. J. Reed, E. J. Tokarsky, Z. Suo, *J. Am. Chem. Soc.* **137**, 5225–5230 (2015).
21. J. A. Cowan, *Chem. Rev.* **98**, 1067–1088 (1998).
22. P. M. Burgers, F. Eckstein, *Proc. Natl. Acad. Sci. U.S.A.* **75**, 4798–4800 (1978).
23. D. Herschlag, J. A. Piccirilli, T. R. Cech, *Biochemistry* **30**, 4844–4854 (1991).
24. C. Biertümpfel *et al.*, *Nature* **465**, 1044–1048 (2010).
25. Y. Su, A. Patra, J. M. Harp, M. Egli, F. P. Guengerich, *J. Biol. Chem.* **290**, 15921–15933 (2015).
26. E. Y. Wu, L. S. Beese, *J. Biol. Chem.* **286**, 19758–19767 (2011).
27. T. N. Kakuda, *Clin. Ther.* **22**, 685–708 (2000).
28. L. P. Jordheim, D. Durantel, F. Zoulim, C. Dumontet, *Nat. Rev. Drug Discov.* **12**, 447–464 (2013).
29. J. Wagner, R. A. Lerner, C. F. Barbas 3rd, *Science* **270**, 1797–1800 (1995).
30. D. N. Bolon, S. L. Mayo, *Proc. Natl. Acad. Sci. U.S.A.* **98**, 14274–14279 (2001).
31. L. Jiang *et al.*, *Science* **319**, 1387–1391 (2008).
32. D. Röthlisberger *et al.*, *Nature* **453**, 190–195 (2008).

ACKNOWLEDGMENTS

Y.G. carried out all experiments; W.Y. conceived and designed the project, and both authors interpreted data and prepared the manuscript. We thank D. J. Leahy and M. Gellert for critical reading and editing the manuscript. This work is funded by NIH intramural program (DK036146-08, W.Y.).

SUPPLEMENTARY MATERIALS

www.sciencemag.org/content/352/6291/1334/suppl/DC1
Materials and Methods
Figs. S1 to S7
Tables S1 to S3
References (*33*–*44*)

8 December 2015; accepted 10 May 2016
10.1126/science.aad9633

CANCER IMMUNOTHERAPY

Targeting of cancer neoantigens with donor-derived T cell receptor repertoires

Erlend Strønen,[1,2] Mireille Toebes,[3] Sander Kelderman,[3] Marit M. van Buuren,[3] Weiwen Yang,[1,2] Nienke van Rooij,[3] Marco Donia,[4] Maxi-Lu Böschen,[1,2] Fridtjof Lund-Johansen,[2,5] Johanna Olweus,[1,2]*† Ton N. Schumacher[3]*†

Accumulating evidence suggests that clinically efficacious cancer immunotherapies are driven by T cell reactivity against DNA mutation–derived neoantigens. However, among the large number of predicted neoantigens, only a minority is recognized by autologous patient T cells, and strategies to broaden neoantigen-specific T cell responses are therefore attractive. We found that naïve T cell repertoires of healthy blood donors provide a source of neoantigen-specific T cells, responding to 11 of 57 predicted human leukocyte antigen (HLA)–A*02:01–binding epitopes from three patients. Many of the T cell reactivities involved epitopes that in vivo were neglected by patient autologous tumor-infiltrating lymphocytes. Finally, T cells redirected with T cell receptors identified from donor-derived T cells efficiently recognized patient-derived melanoma cells harboring the relevant mutations, providing a rationale for the use of such "outsourced" immune responses in cancer immunotherapy.

Accumulating data suggest that tumor regression induced by cancer immunotherapies that exploit the endogenous T cell pool (*1*, *2*) relies on recognition of neoantigens that are formed as a consequence of tumor-specific DNA mutations. A striking observation in cancer patients and in mouse models is that neoantigen-specific T cell reactivity is generally limited to just a few mutant epitopes, even though the number of predicted epitopes is large (*3*–*12*). This scarcity of T cell–recognized neoantigens could potentially reflect immune editing of tumors by T cells (*13*). Alternatively, an effector T cell pool toward many tumor-expressed neoantigens may be absent because of ineffective priming or because of tolerization of these T cells. Recent work has shown that vaccination with neoantigen peptide–loaded dendritic cells can increase the breadth of mutant peptide-specific T cells in melanoma patients (*14*). In that study, it could not be established whether newly induced T cells could recognize autologous tumor cells. Nonetheless, these data provide a further incentive for the development of strategies that broaden neoantigen-specific T cell reactivity.

Here, we aimed to establish whether T cell receptors (TCRs) that are obtained outside of the autologous T cell repertoire can be used to engineer neoantigen-specific T cell immunity. To this end, we generated immune responses to HLA-A*02:01-restricted neoantigens from the non-tolerized T cell repertoires derived from donors that express this allele. Using this approach, we evaluated (i) whether donor-derived T cells can recognize relevant tumor cells, (ii) whether such "outsourced" immune responses provide evidence

[1]Department of Cancer Immunology, Oslo University Hospital Radiumhospitalet, Oslo, Norway. [2]K. G. Jebsen Centers for Cancer Immunotherapy and for Inflammation Research, Institute for Clinical Medicine, University of Oslo, Oslo, Norway. [3]Division of Immunology, Netherlands Cancer Institute, Amsterdam, Netherlands. [4]Center for Cancer Immune Therapy, Department of Hematology, Herlev Hospital, University of Copenhagen, Herlev, Denmark. [5]Department of Immunology and Transfusion Medicine, Oslo University Hospital Rikshospitalet, Oslo, Norway.
***Corresponding author. Email: johanna.olweus@medisin.uio.no (J.O.); t.schumacher@nki.nl (T.N.S.)** †These authors contributed equally to this work.

Science

Capture of a third Mg^{2+} is essential for catalyzing DNA synthesis

Yang Gao and Wei Yang

Science **352** (6291), 1334-1337.
DOI: 10.1126/science.aad9633

A hit-and-run metal ion

DNA polymerase is an enzyme that uses existing DNA as a template to build new DNA by adding new nucleotides to the end of the newly forming daughter strand. The enzyme mechanism that catalyzes formation of a phosphodiester bond is known to require two Mg^{2+} ions, and recent crystal structures have shown that a third metal ion is present after bond formation. Gao *et al.* used time-resolved crystallography to visualize bond formation. The enzyme-substrate complex captures a third cation before bond formation occurs, and DNA synthesis cannot occur without the third metal ion. Binding of this metal ion requires thermal motion of the enzyme-substrate complex, so that catalysis is achieved by acquiring a transient cofactor.

Science, this issue p. 1334